PHYSICAL REVIEW D **95,** 036021 (2017)

Probing new physics in $\overline{B}^0 \to D^{(*)}\tau^-\overline{\nu}_\tau$ using the longitudinal, transverse, and normal polarization components of the tau lepton

M. A. Ivanov,[1,*] J. G. Körner,[2,†] and C. T. Tran[1,3,‡]

[1]*Bogoliubov Laboratory of Theoretical Physics, Joint Institute for Nuclear Research, 141980 Dubna, Russia*

[2]*PRISMA Cluster of Excellence, Institut für Physik, Johannes Gutenberg-Universität, D-55099 Mainz, Germany*

[3]*Department of General and Applied Physics, Moscow Institute of Physics and Technology, 141700 Dolgoprudny, Russia*

(Received 11 January 2017; published 27 February 2017)

We study the longitudinal, transverse, and normal polarization components of the tau lepton in the decays $\overline{B}^0 \to D^{(*)}\tau^-\overline{\nu}_\tau$ and discuss their role in searching for new physics (NP) beyond the standard model (SM). Starting with a model-independent effective Hamiltonian including non-SM four-Fermi operators, we obtain experimental constraints on different NP scenarios and investigate their effects on the polarization observables. In the SM the longitudinal and transverse polarizations of the tau lepton differ substantially from the corresponding zero lepton mass values of $P_L = -1$ and $P_T = 0$. In addition, P_L and P_T are very sensitive to NP effects. For the transverse polarization this holds true, in particular, for the effective tensor operator in the case of $\overline{B}^0 \to D^*$ and for the scalar operator in the case of $\overline{B}^0 \to D$. The T-odd normal polarization P_N, which is predicted to be negligibly small in the SM, can be very sizable assuming NP complex Wilson coefficients. We also discuss in some detail how the three polarization components of the tau lepton can be measured with the help of its subsequent leptonic and semihadronic decays.

DOI: 10.1103/PhysRevD.95.036021

I. INTRODUCTION

The exclusive semileptonic decays $\overline{B}^0 \to D^{(*)}\tau^-\overline{\nu}_\tau$ have been measured by the *BABAR* [1], Belle [2,3], and LHCb [4] collaborations in an effort to unravel the well-known $R_{D^{(*)}}$ puzzle which has persisted for several years [5–34]. Recently, the Belle collaboration reported a new measurement of the decay $\overline{B}^0 \to D^*\tau^-\overline{\nu}_\tau$ using the hadronic τ^- decay modes $\tau^- \to \pi^-\nu_\tau$ and $\tau^- \to \rho^-\nu_\tau$, in which they found $R_{D^*} = 0.270 \pm 0.035(\text{stat})^{+0.028}_{-0.025}(\text{syst})$ [35]. Taking this new result into account, the current world averages of the ratios are $R_D = 0.406 \pm 0.050$ and $R_{D^*} = 0.311 \pm 0.016$, which exceed the SM predictions of $R_D = 0.300 \pm 0.008$ [36–38] and $R_{D^*} = 0.252 \pm 0.003$ [39] by 2.1σ and 3.6σ, respectively.

In Ref. [35] the Belle collaboration also reported on the first measurement of the longitudinal polarization of the tau lepton in the decay $\overline{B}^0 \to D^*\tau^-\overline{\nu}_\tau$ with the result $P_L^\tau = -0.38 \pm 0.51(\text{stat})^{+0.21}_{-0.16}(\text{syst})$. The errors of this measurement are quite large but this pioneering measurement has opened a completely new window on the analysis of the dynamics of the semileptonic $B \to D$ and $B \to D^*$ transitions. The hope is that, with the Belle II super-B factory nearing completion, more precise values of the polarization can be achieved in the future, which would shed more light on the search for possible NP in these decays.

In this paper we shall study the longitudinal, transverse, and normal polarization components of the τ^- in the semileptonic decays $\overline{B}^0 \to D^{(*)}\tau^-\overline{\nu}_\tau$. In order to set up our notation we define three orthogonal unit vectors as follows:

$$\vec{e}_L = \frac{\vec{p}_\tau}{|\vec{p}_\tau|}, \quad \vec{e}_N = \frac{\vec{p}_\tau \times \vec{p}_{D^{(*)}}}{|\vec{p}_\tau \times \vec{p}_{D^{(*)}}|}, \quad \vec{e}_T = \vec{e}_N \times \vec{e}_L, \quad (1)$$

where $\vec{p}_\tau$ and $\vec{p}_{D^{(*)}}$ are the three-momenta of the τ^- and the $D^{(*)}$ meson in the $W^-_{\text{off-shell}}$ rest frame. In the following we shall loosely refer to this frame as the W^- rest frame. The three unit vectors $\vec{e}_T$, $\vec{e}_N$, and $\vec{e}_L$ form a right-handed coordinate system. The longitudinal (L), normal (N), and transverse (T) polarization four-vectors of the τ^- in its rest frame are given by

$$s_L^\mu = (0, \vec{e}_L), \qquad s_N^\mu = (0, \vec{e}_N), \qquad s_T^\mu = (0, \vec{e}_T). \qquad (2)$$

A Lorentz boost from the τ^- rest frame to the W^- rest frame transforms only the longitudinal polarization four-vector according to

*ivanovm@theor.jinr.ru
†jukoerne@uni-mainz.de
‡ctt@theor.jinr.ru, tranchienthang1347@gmail.com

$$s_L^\mu = \left(\frac{|\vec{p}_\tau|}{m_\tau}, \frac{E_\tau}{m_\tau}\frac{\vec{p}_\tau}{|\vec{p}_\tau|}\right), \tag{3}$$

leaving the normal (s_N^μ) and transverse (s_T^μ) polarization four-vectors unchanged. The longitudinal, normal, and transverse polarization components of the tau are given by

$$P_i(q^2) = \frac{d\Gamma(s_i^\mu)/dq^2 - d\Gamma(-s_i^\mu)/dq^2}{d\Gamma(s_i^\mu)/dq^2 + d\Gamma(-s_i^\mu)/dq^2}, \quad i = L, N, T, \tag{4}$$

where $q^\mu = p_B^\mu - p_{D^{(*)}}^\mu$ is the momentum transfer. We note that the terms longitudinal polarization and longitudinal polarization component are often used interchangeably, as in this paper. The same convention is used for the normal and transverse polarizations.

The normal polarization component P_N is a T-odd observable and is predicted to be zero in the SM in the absence of final state interactions which are known to be negligibly small. However, in some extended versions of the SM such as the two-Higgs-doublet models, the minimal supersymmetric standard model, and the leptoquark model, large values of P_N are possible through the introduction of CP-violating phases [40–43].

The longitudinal polarization P_L has also been used as a promising observable in order to probe NP in $\overline{B}^0 \to D^{(*)}\tau^-\overline{\nu}_\tau$ [39,44–48]. P_L has been found to be very sensitive to the scalar and tensor operators. It has been shown in Ref. [44,46] that some correlations between P_L and the decay rate are very useful for NP prediction. In addition, the NP couplings can be extracted from P_L with much less uncertainties as compared to those from other observables [47].

In Ref. [49] we have calculated the SM values of the longitudinal and transverse polarization of the charged lepton in the decays $\overline{B}^0 \to D^{(*)}\ell^-\overline{\nu}_\ell$. The polarization components have been calculated in the so-called helicity basis where the polarization components are given in terms of bilinear forms of the helicity amplitudes of the current-induced $B \to D^{(*)}$ transitions. Depending on the phase space region the transverse tau polarization can become quite large. On average one has $\langle P_T^\tau \rangle = 0.84$ $(B \to D)$ and $\langle P_T^\tau \rangle = 0.46$ $(B \to D^*)$ [49] compared to $\langle P_T^\ell \rangle = 0$ for $m_\ell = 0$ in both cases. For the longitudinal polarization one has $\langle P_L^\tau \rangle = 0.33$ $(B \to D)$ and $\langle P_L^\tau \rangle = -0.50$ $(B \to D^*)$ [49] which one has to compare with the zero lepton mass result $\langle P_L^\ell \rangle = -1$, again in both cases [50]. For the averages of the total polarization $|\vec{P}^\tau|$ one obtains $\langle |\vec{P}^\tau| \rangle = 0.91$ $(B \to D)$ and $\langle |\vec{P}^\tau| \rangle = 0.71$ $(B \to D^*)$. In this paper we also consider the transverse polarization in the presence of NP and compare its NP sensitivity with that of $\langle P_L^\tau \rangle$ and $\langle P_N^\tau \rangle$. The discussion of NP contributions to the transverse and normal polarization components of the τ^- are new.

Since the τ^- lepton decays weakly, its polarization is revealed through its ensuing decay distributions, i.e. it is self-analyzing. As analyzing modes for the τ^- polarization we will consider the four dominant τ^- decay modes

$$\begin{aligned} &\tau^- \to \pi^-\nu_\tau(10.83\%), \qquad &&\tau^- \to \mu^-\overline{\nu}_\mu\nu_\tau(17.41\%), \\ &\tau^- \to \rho^-\nu_\tau(25.52\%), \qquad &&\tau^- \to e^-\overline{\nu}_e\nu_\tau(17.83\%), \end{aligned} \tag{5}$$

where we have added the respective branching fractions in brackets. In the next section, we will show how the three polarization components of the tau can be measured by using its decays as polarization analyzers and how well each mode can serve as polarization analyzer. The remaining parts of the paper are organized as follows: in Sec. III we introduce some formalism concerning the semileptonic transitions, including the derivation of the polarization formulae in the presence of NP. An analysis of NP effects on the polarizations is given in Sec. IV. Finally, we summarize the main results in Sec. V.

II. ANALYZING THE POLARIZATION OF THE TAU THROUGH ITS DECAYS

The polarization components of the τ^- in $\overline{B}^0 \to D^{(*)}\tau^-\overline{\nu}_\tau$ can be measured by using the decay products of the τ^- as polarization analyzers. The kinematics of the decay $\overline{B}^0 \to D^{(*)}\tau^-\overline{\nu}_\tau$ followed by a τ^- decay is depicted in Fig. 1, where $d^- = \pi^-, \rho^-, e^-, \mu^-$. In the W^- rest frame, θ_τ is the angle between the τ^- three-momentum and the direction opposite to the direction of the $D^{(*)}$ meson. In the τ^- rest frame, θ_d is the angle between the three-momentum of the final tau daughter d^- and the longitudinal polarization axis which is chosen to coincide with the direction of the τ^- in the W^- rest frame (helicity basis). The production plane defined by the decay $\overline{B}^0 \to D^{(*)}\tau^-\overline{\nu}_\tau$ is spanned by the three-momenta of the τ^- and the $D^{(*)}$ while the $\tau^- \to d^- + X$ decay plane is spanned by the three-momentum of

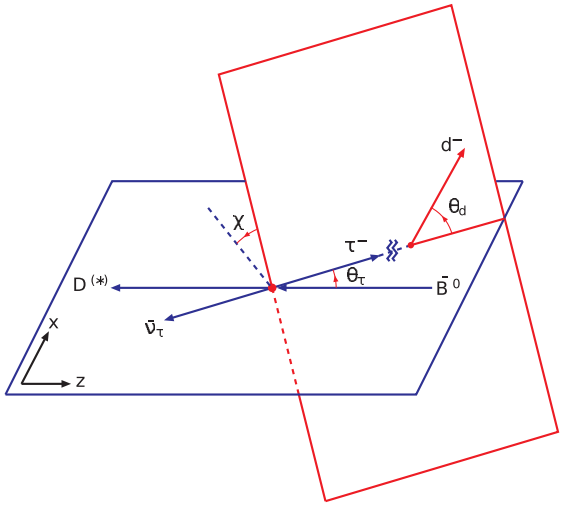

FIG. 1. Kinematics of the decay $\bar{B}^0 \to D^{(*)}\tau^-\bar{\nu}_\tau$ followed by a τ^- decay. See text for more details.

the d^- and the longitudinal polarization axis. The angle χ is the azimuthal angle between the two planes. We choose a right-handed xyz coordinate system in the W^- rest frame such that the z axis is opposite to the direction of the mesons $\overline{B}^0$ and $D^{(*)}$, and the three-momentum of the τ^- lies in the (xz) plane. In this system the τ^- momentum is given by

$$p_\tau^\mu = E_\tau(1, \beta_\tau \sin\theta_\tau, 0, \beta_\tau \cos\theta_\tau), \tag{6}$$

where $E_\tau = (q^2 + m_\tau^2)/2\sqrt{q^2}$ is the energy and $\beta_\tau = |\vec{p}_\tau|/E_\tau = \sqrt{1 - m_\tau^2/E_\tau^2}$ the velocity of the τ^- in the W^- rest frame.

Let us discuss the spin-momentum correlations in the τ^- rest frame. Since we are dealing with two-body decays $(\tau^- \to \pi^-(\rho^-) + \nu_\tau)$ or quasi-two-body decays $(\tau^- \to \ell^- + X)$ there is only one independent spin-momentum scalar product which can be taken to be $(\vec{p}_d \cdot \vec{P})$, where $\vec{p}_d$ is the three-momentum of the d^- and $\vec{P}$ is the polarization vector of the τ^-. Note that in a three-body decay as e.g. in $t \to b + \ell^+ + \nu_\ell$ there are two possible spin-momentum scalars which provide for a richer spin-momentum correlation structure (see e.g. [51,52]). Returning to the two-body decays treated here the differential polar angle distribution is given by

$$\frac{d\Gamma}{dq^2 d\cos\theta_{dP}} = \mathcal{B}_d \frac{d\Gamma}{dq^2} \frac{1}{2}(1 + A_d \cdot |\vec{P}(q^2)| \cos\theta_{dP}), \tag{7}$$

where θ_{dP} is the polar angle between the momentum $\vec{p}_d$ and the polarization vector $\vec{P}$ of the τ^-, and $\mathcal{B}_d$ and A_d are the branching fraction and the analyzing power of the decay $\tau^- \to d^- + X$, respectively. Note that the magnitude of the analyzing power has to satisfy $|A_d| \leq 1$ to guarantee the positivity of rates for $|\vec{P}| = 1$.

The polar angle θ_{dP} appearing in Eq. (7) is experimentally not accessible since the direction of the polarization vector $\vec{P}$ of the τ^- is *a priori* unknown. However, one can define experimentally accessible angles θ_d and χ through the representation of the momentum vector $\vec{p}_d$ in the production plane (see Fig. 1) via

$$\vec{p}_d = |\vec{p}_d|(\sin\theta_d \cos\chi, \sin\theta_d \sin\chi, \cos\theta_d). \tag{8}$$

In terms of the angles θ_d and χ, the decay distribution reads

$$\frac{d\Gamma}{dq^2 d\cos\theta_d d\chi/2\pi} = \mathcal{B}_d \frac{d\Gamma}{dq^2} \frac{1}{2}[1 + A_d(P_T(q^2)\sin\theta_d \cos\chi + P_N(q^2)\sin\theta_d \sin\chi + P_L(q^2)\cos\theta_d)]. \tag{9}$$

Through an analysis of the decay distribution (9) one can determine the three components of the q^2-dependent polarization vector $\vec{P}(q^2) = (P_T(q^2), P_N(q^2), P_L(q^2))$.

Upon χ integration, one obtains

$$\frac{d\Gamma}{dq^2 d\cos\theta_d} = \mathcal{B}_d \frac{d\Gamma}{dq^2} \frac{1}{2}(1 + A_d P_L(q^2)\cos\theta_d) \tag{10}$$

such that the forward-backward polarization asymmetry is given by

$$A_{FB}^P = \frac{d\Gamma(F) - d\Gamma(B)}{d\Gamma(F) + d\Gamma(B)} = A_d P_L(q^2). \tag{11}$$

Upon $\cos\theta_d$ integration one has

$$\frac{d\Gamma}{dq^2 d\chi/2\pi} = \mathcal{B}_d \frac{d\Gamma}{dq^2}\left(1 + A_d \frac{\pi}{4}(P_T(q^2)\cos\chi + P_N(q^2)\sin\chi)\right) \tag{12}$$

with an effective azimuthal analyzing power of $A_d\pi/4$.

A. The semihadronic modes $\tau^- \to \pi^-\nu_\tau$ and $\tau^- \to \rho^-\nu_\tau$

The differential decay rate of $\overline{B}^0 \to D^{(*)}\tau^-(\to \pi^-\nu_\tau)\overline{\nu}_\tau$ reads

$$\frac{d\Gamma_\pi}{dq^2 d\cos\theta_\pi d\chi/2\pi} = \mathcal{B}_\pi \frac{d\Gamma}{dq^2}\frac{1}{2}[1 + P_T(q^2)\sin\theta_\pi\cos\chi + P_N(q^2)\sin\theta_\pi\sin\chi + P_L(q^2)\cos\theta_\pi], \tag{13}$$

where $\mathcal{B}_\pi$ is the branching fraction of $\tau^- \to \pi^-\nu_\tau$ and Γ is the decay rate of $\overline{B}^0 \to D^{(*)}\tau^-\overline{\nu}_\tau$. Note that the analyzing power of the decay $\tau^- \to \pi^-\nu_\tau$ is 100%. In the following we shall drop explicit reference to the component P_N in the angular decay distribution. After $\cos\theta_\pi$ integration, one obtains

$$\frac{d\Gamma_\pi}{dq^2 d\chi/2\pi} = \mathcal{B}_\pi \frac{d\Gamma}{dq^2}\left(1 + \frac{\pi}{4}P_T(q^2)\cos\chi\right). \tag{14}$$

The effective azimuthal analyzing power is quite large with $\pi/4 = 78.54\%$.

For the decay $\overline{B}^0 \to D^{(*)}\tau^-(\to \rho^-\nu_\tau)\overline{\nu}_\tau$ one has

$$\frac{d\Gamma_\rho}{dq^2 d\cos\theta_\rho d\chi/2\pi} = \mathcal{B}_\rho \frac{d\Gamma}{dq^2}\frac{1}{2}\left[1 + \frac{m_\tau^2 - 2m_\rho^2}{m_\tau^2 + 2m_\rho^2}(P_T(q^2)\sin\theta_\rho\cos\chi + P_L(q^2)\cos\theta_\rho)\right], \tag{15}$$

where $\mathcal{B}_\rho$ is the branching fraction of $\tau^- \to \rho^-\nu_\tau$. It is apparent that one looses analyzing power compared

to the case $\tau^- \to \pi^- \nu_\tau$ since $(m_\tau^2 - 2m_\rho^2)/(m_\tau^2 + 2m_\rho^2) = 0.4485 < 1$.

However, one can retain the full analyzing power if one projects out the longitudinal and transverse components of the ρ^-, which can be achieved by an angular analysis of the decay $\rho^- \to \pi^- + \pi^0$ in the rest frame of the ρ^-. The polar angle distribution of the decay $\rho^- \to \pi^- + \pi^0$ reads

$$\frac{d\Gamma_\rho}{d\cos\theta} = \frac{3}{8}(1+\cos^2\theta)\Gamma^T + \frac{3}{4}\sin^2\theta\Gamma^L, \tag{16}$$

where θ is the polar angle of the π^- with respect to the original flight direction of the ρ^-. Technically, one can project out the longitudinal piece of the ρ^- with the help of the normalized longitudinal polarization four-vector of the ρ^- which reads

$$\varepsilon^\alpha(0) = \frac{1}{m_\rho m_\tau p}(m_\rho^2 p_\tau^\alpha - p_\rho p_\tau p_\rho^\alpha). \tag{17}$$

One can check that $p_\rho \cdot \varepsilon(0) = 0$ and that the polarization four-vector is correctly normalized: $\varepsilon^*(0)\cdot\varepsilon(0) = -1$. In the rest frame of the ρ^- one has $\varepsilon^\alpha(0) = (0;0,0,1)$. The transverse contribution can be obtained from the difference $\Gamma^T = \Gamma - \Gamma^L$.

The longitudinal and transverse differential decay distributions of the ρ^- are finally given by

$$\begin{aligned}
\frac{d\Gamma_\rho^L}{dq^2 d\cos\theta_\rho d\chi/2\pi} &= \mathcal{B}_\rho \frac{d\Gamma}{dq^2}\frac{m_\tau^2/2}{m_\tau^2+2m_\rho^2}[1 + (P_T(q^2)\sin\theta_\rho\cos\chi + P_L(q^2)\cos\theta_\rho)],\\
\frac{d\Gamma_\rho^T}{dq^2 d\cos\theta_\rho d\chi/2\pi} &= \mathcal{B}_\rho \frac{d\Gamma}{dq^2}\frac{m_\rho^2}{m_\tau^2+2m_\rho^2}[1 - (P_T(q^2)\sin\theta_\rho\cos\chi + P_L(q^2)\cos\theta_\rho)].
\end{aligned} \tag{18}$$

By separating the two distributions on has regained the full analyzing power of 100% in both cases. This can e.g. be done by projection: $\mathcal{P}^L = 2(1 - 5/2\cos^2\theta)$ will project out the longitudinal and $\mathcal{P}^T = -(1 - 5\cos^2\theta)$ the transverse component. It is evident that the sum of the two distributions (18) gives the result Eq. (15).

B. The leptonic modes $\tau^- \to \ell^- \bar{\nu}_\ell \nu_\tau$ $(\ell = e, \mu)$

Using the results of e.g. Ref. [53], one finds

$$\begin{aligned}
&\frac{d\Gamma_\ell}{dq^2 dx d\cos\theta_\ell d\chi/2\pi}\\
&= \frac{d\Gamma}{dq^2}\frac{\Gamma_0}{\Gamma_\tau}\beta x[G_1(x) + G_2(x)(P_T(q^2)\sin\theta_\ell\cos\chi\\
&\quad + P_L(q^2)\cos\theta_\ell)],
\end{aligned} \tag{19}$$

where, as usual, we have defined a scaled energy variable $x = 2E/m_\tau$ where $E = (|\vec{p}_\ell|^2 + m_\ell^2)^{1/2}$ is the energy of the final charged lepton ℓ^- in the τ^- rest frame. Here, $\Gamma_0 = G_F^2 m_\tau^5/192\pi^3$ is the reference rate for the leptonic decay of final-state massless leptons $m_\ell = 0$, and Γ_τ is the total decay width of the τ^-. Note that the expression to the right of Γ_0/Γ_τ integrates to 1 for $m_\ell = 0$ as it should be. For later purposes we define a reference branching ratio $\mathcal{B}_\ell^0 = \Gamma_0/\Gamma_\tau$.

The coefficient functions in Eq. (19) are given by [53]

$$G_1 = x(3-2x) - (4-3x)y^2, \quad G_2 = \beta x(1 - 2x + 3y^2), \tag{20}$$

where $y = m_\ell/m_\tau$ and $\beta = \sqrt{1-4y^2/x^2} = \sqrt{1-m_\ell^2/E^2} = p/E$. We mention that the next-to-leading order QED radiative corrections to the leptonic polarized τ^- decays can also be found in Ref. [53].

The polar and azimuthal analyzing power is determined by the ratio $G_2(x)/G_1(x)$. By averaging over x $(2y \le x \le 1 + y^2)$, one obtains

$$\frac{\langle \beta x G_2(x)\rangle}{\langle \beta x G_1(x)\rangle} = -\frac{1}{12}(1 + 8y^2 - 32y^3 + \cdots). \tag{21}$$

The azimuthal analyzing power is given by

$$\begin{aligned}
&\frac{d\Gamma_\ell}{dq^2 d\chi/2\pi} = \frac{d\Gamma}{dq^2}\mathcal{B}_\ell^0(1 + P_T A_\chi\cos\chi),\\
&\text{where } A_\chi = -\frac{\pi}{12}(1 + 8y^2 - 32y^3 + \cdots).
\end{aligned} \tag{22}$$

For $m_\ell = 0$ one finds $A_\chi = -0.262$ which increases by 3.2% for $m_\ell = m_\mu$ [see Eq. (22)].

Another possibility to analyze the polarization of the τ^- is to describe the leptonic decay of the polarized τ^- in terms of the variables (x, z), where $z = E_\ell/E_\tau$ is the fractional energy E_ℓ of the daughter lepton and the energy E_τ of the τ^- both in the W^- rest frame [54]. For the dependence $z = z(x, \cos\theta_\ell)$, one finds

$$z = \frac{E_\ell}{E_\tau} = \frac{\beta_\tau p\cos\theta_\ell + E}{m_\tau} = \frac{x}{2}(\beta_\tau\beta\cos\theta_\ell + 1). \tag{23}$$

It is important to realize that E (energy of the daughter lepton in the τ^- rest frame) is no longer fixed but becomes a variable to be integrated over.

Let us first discuss the so-called collinear approximation $\beta_\tau = 1$ and the zero lepton mass limit $\beta = 1$ introduced in Ref. [54] to analyze the longitudinal polarization of the τ^-. The approximation $\beta_\tau = 1$ is good for the small recoil (i.e. large q^2) region. The approximation $\beta = 1$ holds for the limiting case when one can neglect the lepton mass in the final state. With these approximations the twice differential rate reads

$$\frac{d\Gamma_\ell}{dq^2 dx dz d\chi/2\pi} = \mathcal{B}_\ell^0 \frac{d\Gamma}{dq^2} 2(G_1(x) + G_2(x)(P_L \cos\theta_\ell + P_T \sin\theta_\ell \cos\chi)). \quad (24)$$

By integrating Eq. (24) over x in the region $z \le x \le 1$, one obtains

$$\frac{d\Gamma_\ell}{dq^2 dz d\chi/2\pi} = \mathcal{B}_\ell^0 \frac{d\Gamma}{dq^2} \frac{1}{3}(1-z)[(5+5z-4z^2) + P_L(q^2)(1+z-8z^2) - \frac{8}{5} P_T(q^2)\sqrt{z(1-z)}(1+4z)\cos\chi]. \quad (25)$$

The differential rate and the contribution proportional to P_L agree with Eq. (2.8) of Ref. [54]. Upon z integration ($0 \le z \le 1$), one obtains the azimuthal distribution

$$\frac{d\Gamma_\ell}{dq^2 d\chi/2\pi} = \mathcal{B}_\ell^0 \frac{d\Gamma}{dq^2}\left(1 - \frac{\pi}{12} P_T(q^2)\cos\chi\right). \quad (26)$$

The analyzing power is $\pi/12 = 26.18\%$, which is in agreement with the corresponding result in Eq. (22).

The calculation for $\beta_\tau \neq 1$ and $\beta = 1$ is slightly more difficult and has been done by Tanaka and Watanabe [44] for the differential rate and the longitudinal contribution proportional to P_L. The decay distribution in terms of dz is written as

$$\frac{d\Gamma_\ell}{dq^2 dz d\chi/2\pi} = \mathcal{B}_\ell \frac{d\Gamma}{dq^2}[f(q^2,z) + g(q^2,z)P_L(q^2) + h(q^2,z)P_T(q^2)\cos\chi], \quad (27)$$

where $\mathcal{B}_\ell$ is the branching fraction of $\tau^- \to \ell^- \bar{\nu}_\ell \nu_\tau$. Neglecting the lepton mass m_ℓ, i.e. setting $\beta = 1$, the functions f, g, and h are given by

$$f(q^2,z) = \frac{16z^2}{3(1-\beta_\tau^2)^3}[9(1-\beta_\tau^2) - 4(3+\beta_\tau^2)z],$$
$$g(q^2,z) = -\frac{16z^2}{3(1-\beta_\tau^2)^3}\beta_\tau[3(1-\beta_\tau^2) - 16z],$$
$$h(q^2,z) = \frac{4\pi z^2}{(1-\beta_\tau^2)^3}\sqrt{1-\beta_\tau^2}(1-\beta_\tau^2-4z), \quad (28)$$

for $0 \le z \le (1-\beta_\tau)/2$, and

$$f(q^2,z) = \frac{1+\beta_\tau-2z}{3\beta_\tau(1+\beta_\tau)^3}[5(1+\beta_\tau)^2 + 10(1+\beta_\tau)z - 16z^2],$$
$$g(q^2,z) = \frac{1+\beta_\tau-2z}{3\beta_\tau^2(1+\beta_\tau)^3}[(1+\beta_\tau)^2 + 2(1+\beta_\tau)z - 8(1+3\beta_\tau)z^2],$$
$$h(q^2,z) = \frac{4z^2}{(1-\beta_\tau^2)^3}\sqrt{1-\beta_\tau^2}(1-\beta_\tau^2-4z)\left(\frac{\pi}{2} + \arcsin\frac{1-\beta_\tau^2-2z}{2z\beta_\tau}\right) - \frac{\sqrt{\beta_\tau^2-1+4z-4z^2}}{3\beta_\tau^2(1-\beta_\tau^2)^2}[(1-\beta_\tau^2)^2 + 2(1-\beta_\tau^2)z - 8(1+2\beta_\tau^2)z^2], \quad (29)$$

for $(1-\beta_\tau)/2 \le z \le (1+\beta_\tau)/2$. Equations (28) and (29) are obtained by integrating Eq. (24) over x in the regions $2z/(1+\beta_\tau) \le x \le 2z/(1-\beta_\tau)$ and $2z/(1+\beta_\tau) \le x \le 1$, respectively.

In the collinear approximation $\beta_\tau = 1$, the first region $0 \le z \le (1-\beta_\tau)/2$ shrinks to zero, while the second region $(1-\beta_\tau)/2 \le z \le (1+\beta_\tau)/2$ simplifies to $0 \le z \le 1$. The collinear forms of the functions $f(q^2,z)$ and $g(q^2,z)$ in Eq. (25) can be obtained by simply substituting $\beta_\tau = 1$ in Eq. (29). However, it is quite subtle to recover the collinear form of $h(q^2,z)$ in Eq. (25) from Eq. (29) since the treatments of the integral in two cases are different, depending on whether $\beta_\tau = 1$ or $\beta_\tau \neq 1$.

Yet another method to analyze the longitudinal polarization of the τ^- has been suggested in Ref. [55] where a forward-backward asymmetry is defined with respect to $\cos\theta^*$, where θ^* is the angle between the final charged lepton and the recoiling $D^{(*)}$ in the W^- rest system. At the end of this section we shall also discuss a different basis, the so-called off-diagonal basis, where the z axis is chosen to point in the direction of the polarization vector of the τ^-.

C. The off-diagonal basis

In their papers [56–58] Mahlon, Parke, and Shadmi introduced the so-called off-diagonal (OD) basis to maximize spin-spin correlation effects in top quark pair production in e^+e^- and hadronic interactions. As shown in Ref. [59,60] the off-diagonal basis amounts to choosing the z axis to point in the direction of the polarization vector of the top quark, or, in this application, of the polarization vector of the τ^-. For the sake of simplicity, we shall only discuss the off-diagonal basis for the SM case where $P_N = 0$.

The relevant rotation to the off-diagonal basis is achieved by a rotation in the $(\vec{e}_L, \vec{e}_T)$ plane by an angle θ_{OD} where θ_{OD} is the polar angle of the tau polarization relative to the tau three-momentum, measured anticlockwise from the direction of the tau. One has

$$\frac{\sin\theta_{OD}}{\cos\theta_{OD}} = \frac{P_T}{P_L}. \tag{30}$$

In the off-diagonal basis (denoted by a prime), the transverse component of the polarization vector is zero $P'_T = 0$ and the azimuthal contribution proportional to $\cos\chi$ in the angular decay distributions vanishes. Therefore, the sensitivity of the polar angle measurement proportional to $\cos\theta'_d$ is enhanced since $|\vec{P}| = \sqrt{P_T^2 + P_L^2} \geq |P_L|$. Here, θ'_d is the polar angle between the three-momentum of the d^- and the z direction in the off-diagonal basis.

This discussion suggests a possible search strategy to experimentally determine the polarization vector of the τ^- from a set of polar measurements alone. Take a set of directions z in the $(\vec{e}_L, \vec{e}_T)$ plane and maximize the forward-backward polarization asymmetry $A_{FB}^P = A_d P_L(q^2)$ for this set. The z direction corresponding to this maximal value gives the direction of the τ^- polarization vector $\vec{P}$, and the corresponding value of $P_L(q^2)$ obtained from $A_{FB}^P = A_d P_L(q^2)$ determines its magnitude $|\vec{P}|$.

In Fig. 2 we display the q^2 dependence of the angle θ_{OD} for the $B \to D$ and $B \to D^*$ transitions. In the case of the $B \to D$ transition the angle θ_{OD} slightly changes in the range (50°, 70°) for almost the whole q^2 region and quickly decreases from 50° to 0° for $q^2 \gtrsim 10$ GeV^2. In the case of the $B \to D^*$ transition the angle θ_{OD} monotonically increases with q^2 from about 80° to 180°.

The q^2 dependence of the angle θ_{OD} is obviously related to the correlation between the longitudinal and transverse polarization components, or in other words, the orientation and the length of the polarization vector. In Fig. 3 we show how the apex of the polarization vector moves in the (P_L, P_T) plane when q^2 increases from threshold $q^2 = m_\tau^2$ to the zero-recoil points $q^2 = (m_{\overline{B}^0} - m_{D^{(*)}})^2$. The apexes move within the unit circle since $|\vec{P}| \leq 1$. Both trajectories start off at threshold and end up at the zero-recoil points. As

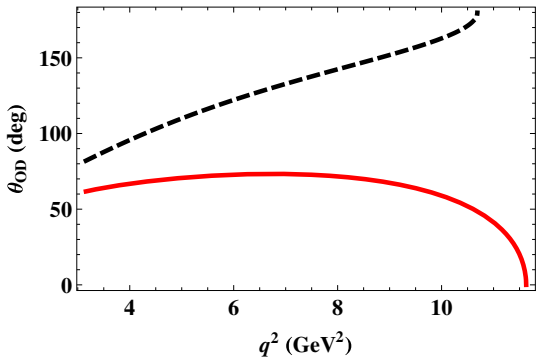

FIG. 2. The angle θ_{OD} for the $B \to D^*$ (dashed line) and $B \to D$ (solid line) transitions.

q^2 increases, the polarization vector of the τ^- turns into the direction of its three-momentum (for the $B \to D$ transition) or opposite to it (for the $B \to D^*$ transition). Both transverse polarization components vanish at zero recoil as follows from the helicity analysis in Sec. III. It is interesting to note that, in the case of the $B \to D^*$ transition, the dots are approximately equally spaced on the trajectory, which indicates a moderate rotation of the polarization vector when q^2 increases. In contrast, the polarization vector in the case of the $B \to D$ transition rotates quite fast for $q^2 \gtrsim 10$ GeV^2. These behaviors are also reflected in the q^2 dependence of the angle θ_{OD} shown in Fig. 2. The average values of the polar angle θ_{OD} read $\langle\theta_{OD}\rangle = 130°$ for $B \to D^*$ and $\langle\theta_{OD}\rangle = 64°$ for $B \to D$.

III. EFFECTIVE OPERATORS AND HELICITY AMPLITUDES

Assuming that all neutrinos are left-handed and that NP effects only influence leptons of the third generation, the effective Hamiltonian for the quark-level transition $b \to c\tau^-\overline{\nu}_\tau$ is given by

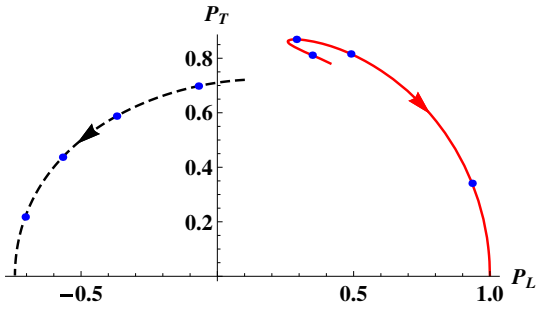

FIG. 3. The q^2 dependence of the orientation and the length of the polarization vector for the $B \to D^*$ (dashed line) and $B \to D$ (solid line) transitions. The arrows show the direction of increasing q^2. The dots on the dashed line stand for $q^2 = 4$, 6, 8, and 10 GeV^2. The dots on the solid line stand for $q^2 = 4$, 8, 10, and 11.5 GeV^2.

$$\mathcal{H}_{\rm eff} = \frac{4G_F}{\sqrt{2}} V_{cb} \left[\mathcal{O}_{V_L} + \sum_{X=S_L,S_R,V_L,V_R,T_L} X \mathcal{O}_X \right], \tag{31}$$

where the four-Fermi operators $\mathcal{O}_X$ are defined as

$$\begin{aligned}
\mathcal{O}_{V_L} &= (\bar{c}\gamma^\mu P_L b)(\bar{\tau}\gamma_\mu P_L \nu_\tau), \\
\mathcal{O}_{V_R} &= (\bar{c}\gamma^\mu P_R b)(\bar{\tau}\gamma_\mu P_L \nu_\tau), \\
\mathcal{O}_{S_L} &= (\bar{c} P_L b)(\bar{\tau} P_L \nu_\tau), \\
\mathcal{O}_{S_R} &= (\bar{c} P_R b)(\bar{\tau} P_L \nu_\tau), \\
\mathcal{O}_{T_L} &= (\bar{c}\sigma^{\mu\nu} P_L b)(\bar{\tau}\sigma_{\mu\nu} P_L \nu_\tau),
\end{aligned} \tag{32}$$

and X's are the NP complex Wilson coefficients which are equal to zero in the SM.

The invariant form factors describing the hadronic transitions $\overline{B}^0 \to D$ and $\overline{B}^0 \to D^*$ are defined as follows:

$$\begin{aligned}
\langle D(p_2)|\bar{c}\gamma^\mu b|\overline{B}^0(p_1)\rangle &= F_+(q^2)P^\mu + F_-(q^2)q^\mu, \\
\langle D(p_2)|\bar{c} b|\overline{B}^0(p_1)\rangle &= (m_1+m_2)F^S(q^2), \\
\langle D(p_2)|\bar{c}\sigma^{\mu\nu}(1-\gamma^5)b|\overline{B}^0(p_1)\rangle &= \frac{iF^T(q^2)}{m_1+m_2}(P^\mu q^\nu - P^\nu q^\mu + i\varepsilon^{\mu\nu Pq}), \\
\langle D^*(p_2)|\bar{c}\gamma^\mu(1\mp\gamma^5)b|\overline{B}^0(p_1)\rangle &= \frac{\epsilon^\dagger_{2\alpha}}{m_1+m_2}[\mp g^{\mu\alpha} Pq A_0(q^2) \pm P^\mu P^\alpha A_+(q^2) \\
&\quad \pm q^\mu P^\alpha A_-(q^2) + i\varepsilon^{\mu\alpha Pq} V(q^2)], \\
\langle D^*(p_2)|\bar{c}\gamma^5 b|\overline{B}^0(p_1)\rangle &= \epsilon^\dagger_{2\alpha} P^\alpha G^S(q^2), \\
\langle D^*(p_2)|\bar{c}\sigma^{\mu\nu}(1-\gamma^5)b|\overline{B}^0(p_1)\rangle &= -i\epsilon^\dagger_{2\alpha}\Big[(P^\mu g^{\nu\alpha} - P^\nu g^{\mu\alpha} + i\varepsilon^{P\mu\nu\alpha})G_1^T(q^2) + (q^\mu g^{\nu\alpha} - q^\nu g^{\mu\alpha} + i\varepsilon^{q\mu\nu\alpha})G_2^T(q^2) \\
&\quad + (P^\mu q^\nu - P^\nu q^\mu + i\varepsilon^{Pq\mu\nu})P^\alpha \frac{G_0^T(q^2)}{(m_1+m_2)^2}\Big],
\end{aligned} \tag{33}$$

where $P = p_1 + p_2$, $q = p_1 - p_2$, and ϵ_2 is the polarization vector of the D^* meson which satisfies the condition $\epsilon_2^\dagger \cdot p_2 = 0$. The particles are on their mass shells: $p_1^2 = m_1^2 = m_{\overline{B}^0}^2$ and $p_2^2 = m_2^2 = m_{D^{(*)}}^2$.

Using the helicity technique first described in Refs. [61–63] and further discussed in our recent papers [5,49] one obtains the ratio of branching fractions $R_{D^{(*)}}(q^2)$ as follows:

$$R_{D^{(*)}}(q^2) = \left(\frac{q^2 - m_\tau^2}{q^2 - m_\mu^2}\right)^2 \frac{\mathcal{H}_{\rm tot}^{D^{(*)}}}{\sum_n |H_n|^2 + \delta_\mu(\sum_n |H_n|^2 + 3|H_t|^2)}, \tag{34}$$

where

$$\begin{aligned}
\mathcal{H}_{\rm tot}^D &= |1+g_V|^2[|H_0|^2 + \delta_\tau(|H_0|^2 + 3|H_t|^2)] + \frac{3}{2}|g_S|^2|H_P^S|^2 \\
&\quad + 3\sqrt{2\delta_\tau}\,{\rm Re} g_S H_P^S H_t + 8|T_L|^2(1+4\delta_\tau)|H_T|^2 + 12\sqrt{2\delta_\tau}\,{\rm Re} T_L H_0 H_T,
\end{aligned} \tag{35}$$

$$\mathcal{H}^{D^*}_{\rm tot} = (|1+V_L|^2+|V_R|^2)\left[\sum_n |H_n|^2 + \delta_\tau\left(\sum_n |H_n|^2 + 3|H_t|^2\right)\right] + \frac{3}{2}|g_P|^2|H_V^S|^2$$
$$- 2{\rm Re}V_R[(1+\delta_\tau)(|H_0|^2+2H_+H_-) + 3\delta_\tau|H_t|^2] - 3\sqrt{2\delta_\tau}{\rm Re}g_P H_V^S H_t$$
$$+ 8|T_L|^2(1+4\delta_\tau)\sum_n |H_T^n|^2 - 12\sqrt{2\delta_\tau}{\rm Re}T_L\sum_n H_n H_T^n. \quad (36)$$

Here, $\delta_\ell = m_\ell^2/2q^2$ is the helicity flip factor, $g_V \equiv V_L + V_R$, $g_S \equiv S_L + S_R$, $g_P \equiv S_L - S_R$, and the index n runs through $(0,+,-)$. The definition of the hadronic helicity amplitudes in terms of the invariant form factors are presented in the Appendix. The expressions for $\mathcal{H}^{D^{(*)}}_{\rm tot}$ in Eqs. (35) and (36) agree with the results of Ref. [14]. Note that in this paper we do not consider interference terms between different NP operators since we assume the dominance of only one NP operator besides the SM contribution.

In the remaining part of this section, we provide the formulae for the polarization components of the τ^- including NP contributions. Starting from the definition given in Eq. (4) one easily obtains the differential decay rate for a given spin projection in a given direction by using the Dirac projection operators, which results in the replacement of

$$\not{p}_\tau + m_\tau \to \frac{1}{2}(\not{p}_\tau + m_\tau)(1+\gamma_5 \not{s}_i) \quad (37)$$

in the relevant traces. The W^- rest frame polarization vectors s_i^μ are given by [64–66]

$$s_L^\mu = \frac{1}{m_\tau}(|\vec{p}_\tau|, E_\tau \sin\theta_\tau, 0, E_\tau\cos\theta_\tau),$$
$$s_T^\mu = (0, \cos\theta_\tau, 0, -\sin\theta_\tau),$$
$$s_N^\mu = (0,0,1,0). \quad (38)$$

The longitudinal polarization reads

$$P_L^D(q^2) = \frac{1}{\mathcal{H}^D_{\rm tot}}\{-|1+g_V|^2[|H_0|^2 - \delta_\tau(|H_0|^2+3|H_t|^2)] + 3\sqrt{2\delta_\tau}{\rm Re}g_S H_P^S H_t$$
$$+ \frac{3}{2}|g_S|^2|H_P^S|^2 + 8|T_L|^2(1-4\delta_\tau)|H_T|^2 - 4\sqrt{2\delta_\tau}{\rm Re}T_L H_0 H_T\},$$
$$P_L^{D^*}(q^2) = \frac{1}{\mathcal{H}^{D^*}_{\rm tot}}\left\{(|1+V_L|^2+|V_R|^2)\left[-\sum_n |H_n|^2 + \delta_\tau\left(\sum_n |H_n|^2 + 3|H_t|^2\right)\right]\right.$$
$$- 2{\rm Re}V_R[(1-\delta_\tau)(-|H_0|^2+2H_+H_-) + 3\delta_\tau|H_t|^2] - 3\sqrt{2\delta_\tau}{\rm Re}g_P H_V^S H_t$$
$$\left. + \frac{3}{2}|g_P|^2|H_V^S|^2 + 8|T_L|^2(1-4\delta_\tau)\sum_n |H_T^n|^2 + 4\sqrt{2\delta_\tau}{\rm Re}T_L\sum_n H_n H_T^n\right\}. \quad (39)$$

We emphasize that the longitudinal polarization of the τ^- is defined in the W^- rest frame with $\vec{p}_\tau$ defining the longitudinal direction, and not in the rest frame of the parent $\overline{B}^0$ meson.

Similarly, the transverse polarization is given by

$$P_T^D(q^2) = \frac{3\pi\sqrt{\delta_\tau}}{2\sqrt{2}\mathcal{H}^D_{\rm tot}}\left\{|1+g_V|^2 H_0 H_t + \frac{{\rm Re}g_S}{\sqrt{2\delta_\tau}}H_P^S H_0 + 4\sqrt{2\delta_\tau}{\rm Re}T_L H_t H_T\right\},$$
$$P_T^{D^*}(q^2) = \frac{3\pi\sqrt{\delta_\tau}}{4\sqrt{2}\mathcal{H}^{D^*}_{\rm tot}}\left\{(|1+V_L|^2-|V_R|^2)(|H_-|^2-|H_+|^2) + 2(|1+V_L|^2+|V_R|^2)H_t H_0\right.$$
$$- \frac{2{\rm Re}g_P}{\sqrt{2\delta\tau}}H_V^S H_0 - 4{\rm Re}V_R H_t H_0 + 16|T_L|^2(|H_T^-|^2 - |H_T^+|^2)$$
$$\left. + 4{\rm Re}T_L\left[\frac{1+2\delta_\tau}{\sqrt{2\delta_\tau}}(H_+H_T^+ - H_-H_T^-) - 2\sqrt{2\delta_\tau}H_t H_T^0\right]\right\}. \quad (40)$$

TABLE I. Parameters of the dipole approximation in Eq. (42) for $\bar{B}^0 \to D^{(*)}$ form factors. Zero-recoil values of the form factors are also listed for comparison with the HQET.

	$\bar{B}^0 \to D^*$								$\bar{B}^0 \to D$			
	A_0	A_+	A_-	V	G^S	G_0^T	G_1^T	G_2^T	F_+	F_-	F^S	F^T
$F(0)$	1.62	0.67	−0.77	0.77	−0.50	−0.073	0.73	−0.37	0.79	−0.36	0.80	0.77
a	0.34	0.87	0.89	0.90	0.87	1.23	0.90	0.88	0.75	0.77	0.22	0.76
b	−0.16	0.057	0.070	0.075	0.060	0.33	0.074	0.065	0.039	0.046	−0.098	0.043
$F(q^2_{\rm max})$	1.91	0.99	−1.15	1.15	−0.74	−0.13	1.10	−0.55	1.14	−0.53	0.89	1.11
$F^{\rm HQET}(q^2_{\rm max})$	1.99	1.12	−1.12	1.12	−0.62	0	1.12	−0.50	1.14	−0.54	0.88	1.14

As can be seen directly from Eq. (40), the transverse polarization vanishes in the zero lepton mass limit $m_\ell = 0$ due to the overall factor $\sqrt{\delta_\ell} = m_\ell/\sqrt{2q^2}$. Physically, this comes about since the lepton is 100% longitudinally polarized for $m_\ell = 0$ and thus there is no room for a transverse polarization. It is the lepton mass that brings in the transverse polarization which, in fact, is quite large in the case of the τ^-. In the SM the transverse polarization can be seen to vanish at zero recoil as a result of the zero-recoil relations $H_t = 0$ and $H_\pm = H_0$ (see the Appendix).

The normal polarization is zero in the SM because we take the form factors and thereby the helicity amplitudes to be real. In the presence of NP *CP*-violating complex Wilson coefficients, they obtain nonzero contributions from the imaginary part of the coefficients as can be seen in Eq. (41). Both P_N^D and $P_N^{D^*}$ are sensitive to the tensor and scalar operators. The normal polarization reads

$$P_N^D(q^2) = \frac{3\pi}{2\mathcal{H}_{\rm tot}^D}[-{\rm Im}g_S H_P^S H_0 + 8\delta_\tau {\rm Im}T_L H_t H_T],$$
$$P_N^{D^*}(q^2) = \frac{3\pi}{4\mathcal{H}_{\rm tot}^{D^*}}\{{\rm Im}g_P H_V^S H_0 - 2{\rm Im}T_L[(1-2\delta_\tau)(H_+ H_T^+ - H_- H_T^-) + 4\delta\tau H_t H_T^0]\}. \quad (41)$$

IV. NUMERICAL ANALYSIS

It is important to note that all the discussions and expressions that we have provided so far are model independent. Now, in order to make numerical predictions we use the form factors calculated in the covariant confined quark model (CCQM) [5] which has been developed in several previous papers by our group (see Refs. [67–69] and references therein). One can also employ the form factors obtained from the heavy quark effective theory

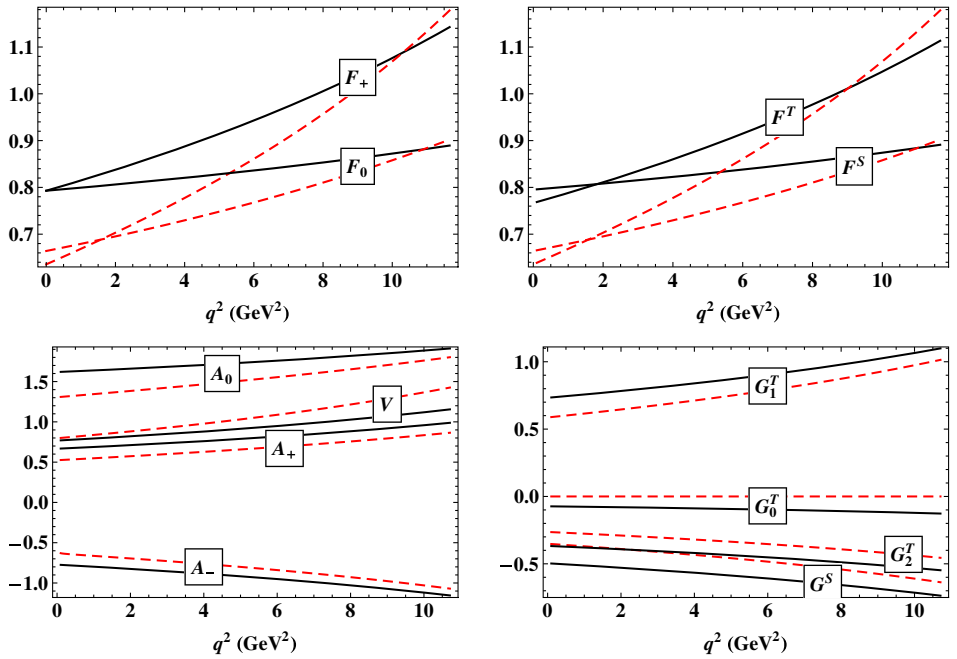

FIG. 4. Comparison of our form factors (solid lines) with the AKC form factors [55] (dashed lines) for the $\bar{B}^0 \to D$ (upper panels) and $\bar{B}^0 \to D^*$ (lower panels) transitions. Each CCQM form factor is labeled together with the corresponding AKC one by a box with their name put on both lines.

(HQET) with better controlled errors. However, in this section, we only aim at clarifying the role of the tau polarization in searching for NP; therefore, the use of our form factors is well suited. For example, the longitudinal polarizations calculated in our model assuming only the SM operator are $\langle P_L^D \rangle = 0.33$ and $\langle P_L^{D^*} \rangle = -0.50$, which are in very good agreement with other results in the literature $\langle P_L^D \rangle = 0.325 \pm 0.009$ [44] and $\langle P_L^{D^*} \rangle = -0.497 \pm 0.013$ [35,46].

A. Form factors in the CCQM

As has been discussed in detail in Ref. [5] we calculate the current-induced $B \to D^{(*)}$ transitions from their one-loop quark diagrams. As a result the various form factors in our model are represented by three-fold integrals which are calculated by using FORTRAN codes in the full kinematical momentum transfer region $0 \le q^2 \le q^2_{\rm max} = (m_{\overline{B}^0} - m_{D^{(*)}})^2$. Our numerical results for the form factors are well represented by a double-pole parametrization

$$F(q^2) = \frac{F(0)}{1 - as + bs^2}, \qquad s = \frac{q^2}{m_1^2}. \tag{42}$$

The parameters of the form factors for the $\overline{B}^0 \to D$ and $\overline{B}^0 \to D^*$ transitions are listed in Table I. We also list the zero-recoil values of the form factors for comparison with the corresponding HQET results which can e.g. be found in Ref. [5]. The agreement between the two sets of zero-recoil values is within 10%. It is worth mentioning that we obtain a nonzero result for the form factor G_0^T at zero recoil, which is predicted to vanish in the HQET.

In Fig. 4, we compare our form factors with the Alonso-Kobach-Camalich (AKC) form factors calculated in Ref. [55] where they have used theoretical input from the HQET, lattice calculations, and equation of motion (EOM) relations. We rewrite the AKC form factors in our notation using the relations between the two sets of form factors. The form factor $F_0(q^2)$ in Fig. 4 is given by

$$F_0(q^2) = F_+(q^2) + \frac{q^2}{m_1^2 - m_2^2} F_-(q^2). \tag{43}$$

It is seen that our form factors share quite similar shapes with the corresponding AKC ones. The first plot in Fig. 4 shows that our form factors $F_+(q^2)$ and $F_0(q^2)$ (solid lines) satisfy the relation $F_0(0) = F_+(0)$ while the corresponding

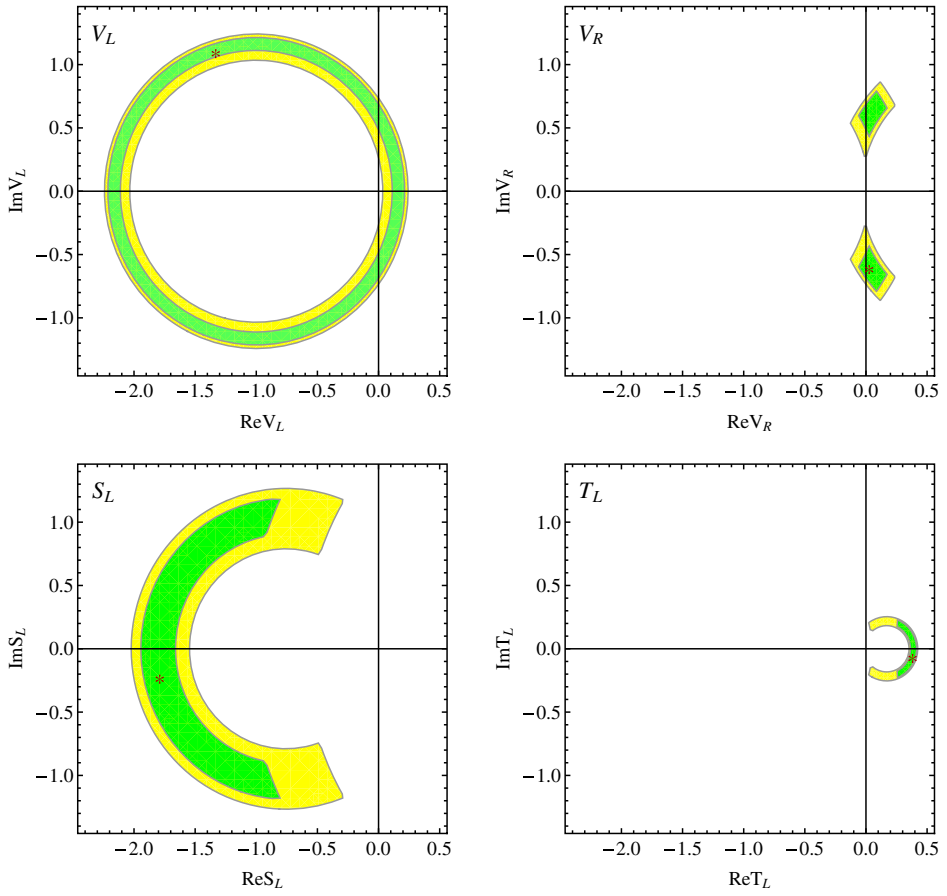

FIG. 5. Constraints on the Wilson coefficients V_L, V_R, S_L, and T_L within 1σ (green, dark) and 2σ (yellow, light). No value of S_R is allowed within 2σ. The best-fit value in each case is denoted with the symbol $*$.

AKC form factors (dashed lines) are slightly different at $q^2 = 0$. This is due to the fact that in their paper [55], the authors used different parametrizations for $F_+(q^2)$ and $F_0(q^2)$. More specifically, they used the Caprini-Lellouch-Neubert parametrization for $F_+(q^2)$ [46,70], but the Bourrely-Caprini-Lellouch parametrization for $F_0(q^2)$ [36,71]. However, the difference $F_0(0) - F_+(0) \approx 0.03$ lies within the uncertainty of $F_+(q^2)$ at $q^2 = 0$, which reads $F_+(0) = 0.664(34)$ [36].

We note that in Ref. [49] the heavy quark limit (HQL) in our approach was explored in great detail for the heavy-to-heavy $\overline{B}^0 \to D^{(*)}$ transitions. In Ref. [49] we also calculated the Isgur-Wise function and considered the near-recoil behavior of the form factors. A brief discussion of the subleading corrections to the HQL arising from finite quark masses can be found in Appendix B of our paper [5]. Note that our form factors do not satisfy the EOM relations since the b and c quarks in the relevant propagators in the quark loop are off their mass shells.

Finally, we briefly discuss some error estimates within our model. We fix our model parameters (the constituent quark masses, the infrared cutoff, and the hadron size parameters) by minimizing the functional $\chi^2 = \sum_i \frac{(y_i^{\rm expt} - y_i^{\rm theor})^2}{\sigma_i^2}$ where σ_i is the experimental uncertainty. If σ is too small then we take its value of 10%. Moreover, we observed that the errors of the fitted parameters are of the order of 10%. Thus we estimate the model uncertainties to lie within 10%.

B. Experimental constraints

Within the SM (without any NP operators) our model calculation yields $R(D) = 0.267$ and $R(D^*) = 0.238$, which are consistent with other SM predictions given in Refs. [36–39] within 10%. Assuming the dominance of only one NP operator in Eq. (31) at a time (besides the SM contribution), we compare the calculated ratios $R_{D^{(*)}}$ with the current experimental data $R_D = 0.406 \pm 0.050$ and $R_{D^*} = 0.311 \pm 0.016$ given in Sec. I and obtain the allowed regions for the NP couplings as shown in Fig. 5. It is important to note that while determining these regions, we also take into account a theoretical error of 10% for the ratios $R(D^{(*)})$. The operator $\mathcal{O}_{S_R}$ is excluded at 2σ and is not presented here. The operator $\mathcal{O}_{V_L}$ is not excluded, but it does not affect the polarizations in general and, therefore, will not be considered in what follows. In other words, only

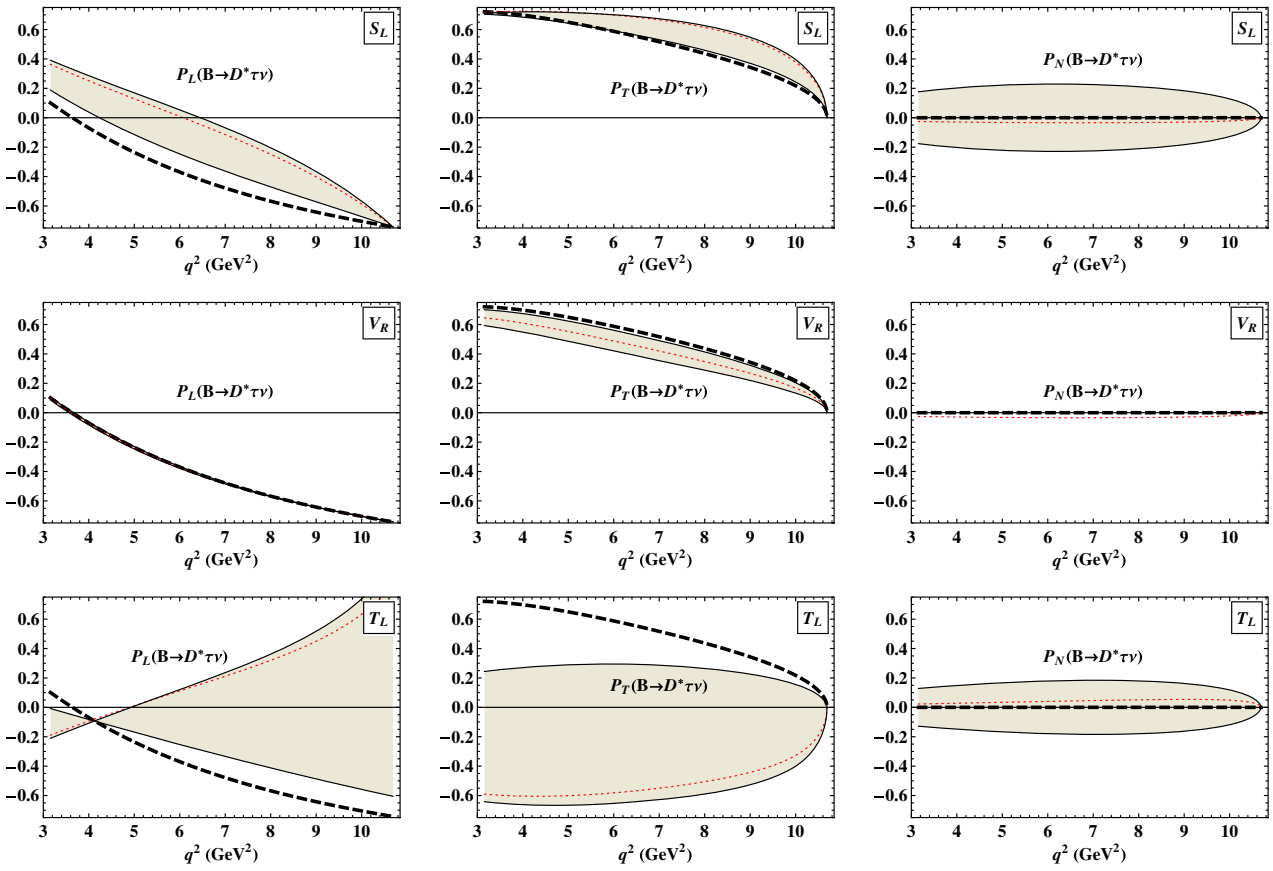

FIG. 6. Longitudinal (left), transverse (center), and normal (right) polarization of the τ^- in the decay $\bar{B}^0 \to D^*\tau^-\bar{\nu}_\tau$. The thick black dashed lines are the SM prediction; the gray bands include NP effects corresponding to the 2σ allowed regions in Fig. 5; the red dotted lines represent the best-fit values of the NP couplings given in Eq. (44).

three NP operators $\mathcal{O}_{V_R}$, $\mathcal{O}_{S_L}$, and $\mathcal{O}_{T_L}$ can modify the polarizations. In each allowed region at 2σ we find the best-fit value for each NP coupling. The best-fit couplings read

$$V_L = -1.33 + i1.11, \qquad V_R = 0.03 - i0.60,$$
$$S_L = -1.79 - i0.22, \qquad T_L = 0.38 - i0.06, \tag{44}$$

and are marked with an asterisk.

C. Theoretical predictions

The τ^- polarization components in $\overline{B}^0 \to D^*\tau^-\overline{\nu}_\tau$ are shown in Fig. 6. In each column we present one component in the presence of different NP couplings S_L, V_R, and T_L, one by one. In each row one can see how one NP coupling affects the three components at the same time. All the plots are in one scale so that one can quickly compare the sensitivity of different polarization components to different NP couplings.

Let us begin with the longitudinal polarization (left column in Fig. 6). The longitudinal polarization $P_L^{D^*}$ is not affected by V_R but is very sensitive to S_L and T_L. Both S_L and T_L tend to increase $P_L^{D^*}$ and shift the zero-crossing point from that in the SM. In the presence of S_L, $P_L^{D^*}$ starts at a higher value but converges to its SM value at high q^2 and its shape is similar to the SM one. In contrast to S_L, T_L changes $P_L^{D^*}$ thoroughly: $P_L^{D^*}$ now starts at a lower position but can be positive for the most part of the whole q^2 region and maximally diverts from its SM prediction at high q^2.

The transverse polarization $P_T^{D^*}$ (center column in Fig. 6) has the same sensitivity to S_L and V_R but S_L tends to increase $P_T^{D^*}$ while V_R tends to decrease $P_T^{D^*}$. The transverse polarization is extremely sensitive to T_L and its sign can be changed in the presence of T_L. It is interesting to note that S_L increases both $P_L^{D^*}$ and $P_T^{D^*}$, while T_L amplifies $P_L^{D^*}$ but lowers $P_T^{D^*}$. When T_L is present, largest deviations of $P_T^{D^*}$ from its SM prediction happen at low q^2, which is opposite to the case of $P_L^{D^*}$.

Regarding the normal polarization $P_N^{D^*}$ (right column in Fig. 6), it is sensitive to both S_L and T_L but slightly more to S_L. $P_N^{D^*}$ can be both positive or negative and its absolute value can reach about 0.2. It is worth noting that $P_N^{D^*}$ is much less sensitive to T_L in comparison with $P_L^{D^*}$ and $P_T^{D^*}$.

Next we turn to the τ^- polarizations in $\overline{B}^0 \to D\tau^-\overline{\nu}_\tau$, which are shown in Fig. 7. It is readily seen that all three polarization components in this case are much more sensitive to S_L than to T_L. In the presence of T_L, the polarizations P_L^D and P_T^D can be positively or negatively enhanced but their shapes over the whole q^2 range are similar to those in the SM. In contrast, the scalar coupling S_L changes the shapes of P_L^D and P_T^D dramatically and can even imply a zero-crossing point, which is impossible in the SM. This distinct effect of S_L may give some hints for experimental study. The normal polarization P_N^D can reach about ± 0.2 under the effect of T_L while it can even reach about ± 0.8 when S_L is present.

The q^2 dependence of the polarizations bears powerful information for discriminating between different NP scenarios. One possible approach is to make use of it to perform a bin-by-bin analysis in order to probe NP in different q^2 regions. One can also calculate the average polarizations over the whole q^2 region. When calculating the q^2 averages, one has to multiply the numerator and denominator of (39), (40), and (41) by the q^2-dependent

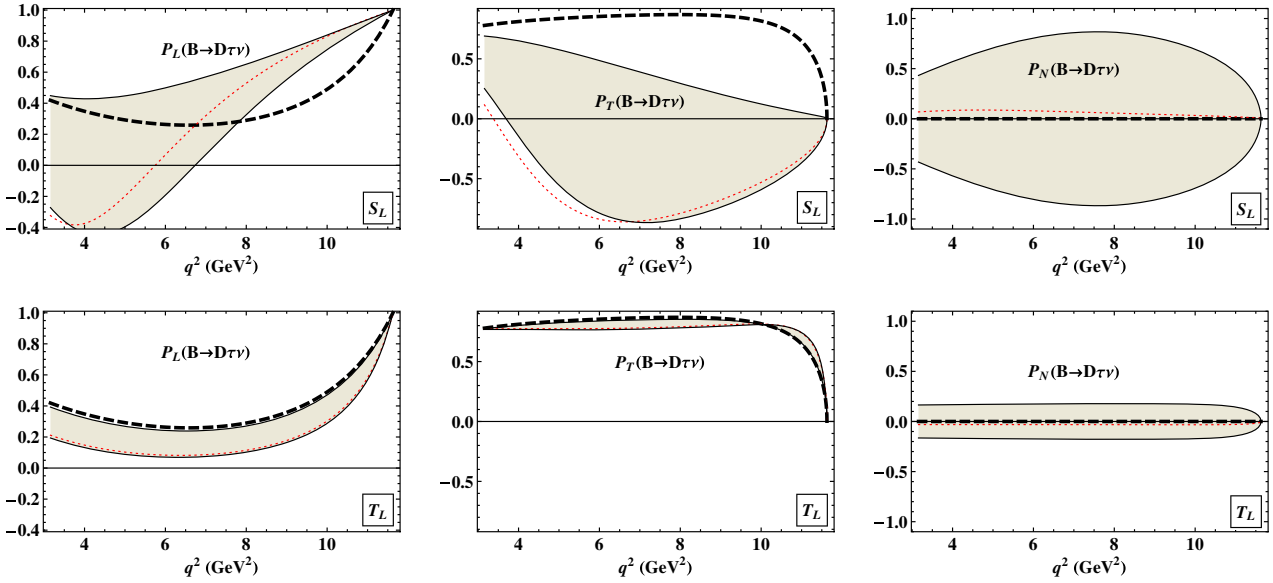

FIG. 7. Longitudinal (left), transverse (center), and normal (right) polarization of the τ^- in the decay $\bar{B}^0 \to D\tau^-\bar{\nu}_\tau$. Notations are the same as in Fig. 6.

TABLE II. q^2 averages of the polarization components and the total polarization. The two rows labeled by SM (CCQM) contain our predictions using SM effective operators with transition form factors calculated in the CCQM. The predicted intervals for the observables in the presence of NP are given in correspondence with the 2σ allowed regions of the NP couplings depicted in Fig. 5.

$\bar{B}^0 \to D$				
	$\langle P_L^D \rangle$	$\langle P_T^D \rangle$	$\langle P_N^D \rangle$	$\langle \lvert \vec{P}^D \rvert \rangle$
SM (CCQM)	0.33	0.84	0	0.91
S_L	(0.36,0.67)	$(-0.68, 0.33)$	$(-0.76, 0.76)$	(0.89,0.96)
T_L	(0.13,0.31)	(0.78,0.83)	$(-0.17, 0.17)$	(0.79,0.90)
$\bar{B}^0 \to D^*$				
	$\langle P_L^{D^*} \rangle$	$\langle P_T^{D^*} \rangle$	$\langle P_N^{D^*} \rangle$	$\langle \lvert \vec{P}^{D^*} \rvert \rangle$
SM (CCQM)	−0.50	0.46	0	0.71
S_L	$(-0.40, -0.14)$	(0.47,0.62)	$(-0.20, 0.20)$	(0.69,0.70)
T_L	$(-0.36, 0.24)$	$(-0.61, 0.26)$	$(-0.17, 0.17)$	(0.23,0.69)
V_R	−0.50	(0.32,0.43)	0	(0.48,0.67)

piece of the phase-space factor given by $C(q^2) = |\mathbf{p_2}|(q^2 - m_\tau^2)^2/q^2$, where $|\mathbf{p_2}| = \lambda^{1/2}(m_1^2, m_2^2, q^2)/2m_1$ is the momentum of the daughter meson. For example, the average longitudinal polarization $\langle P_L^D \rangle$ can then be calculated according to

$$\langle P_L^D \rangle = \frac{\int dq^2 C(q^2)(P_L^D(q^2)\mathcal{H}_{\rm tot}^D)}{\int dq^2 C(q^2)\mathcal{H}_{\rm tot}^D}. \tag{45}$$

The predictions for the mean polarizations are summarized in Table II. Again, one sees that the τ^- polarization components in $\overline{B}^0 \to D\tau^-\overline{\nu}_\tau$ are extremely sensitive to S_L. When S_L is present, $\langle P_L^D \rangle$ can be as large as 0.67, $\langle P_T^D \rangle$ can reach −0.68, and $\langle P_N^D \rangle$ can even reach ± 0.76. It is interesting to note that if one measures $\langle P_L^D \rangle$ and finds any excess over the SM value, it would be a clear sign of S_L. Meanwhile, the τ^- longitudinal and transverse polarization components in $\overline{B}^0 \to D^*\tau^-\overline{\nu}_\tau$ are more sensitive to T_L. The coupling T_L can enhance $\langle P_L^{D^*} \rangle$ from the SM value of −0.50 up to 0.24, or lower $\langle P_T^{D^*} \rangle$ from 0.46 down to −0.61. Notably, the average transverse polarization $\langle P_T^D \rangle$ is almost insensitive to T_L in comparison with S_L. When T_L is present, one finds $0.78 \le \langle P_T^D \rangle \le 0.83$, which is almost the same as the SM value $\langle P_T^D \rangle = 0.84$. In contrast, if S_L is present, one has $-0.68 \le \langle P_T^D \rangle \le 0.33$, which is much lower than the SM prediction. This unique property of $\langle P_T^D \rangle$ may play a very important role in probing the scalar coupling S_L. It is also interesting to note that the average total polarization $\langle |\vec{P}^{D^*}| \rangle$ is almost insensitive to S_L.

V. SUMMARY AND CONCLUSIONS

We have studied the longitudinal, transverse, and normal polarization components of the τ^- in the semileptonic decays $\overline{B}^0 \to D^{(*)}\tau^-\overline{\nu}_\tau$ in the presence of NP scalar, vector, and tensor interactions based on an SM-extended effective Hamiltonian. Constraints on the space of NP couplings have been obtained from experiments at B factories and LHCb including the most recent result of the Belle collaboration [35]. We have also briefly discussed how to extract the polarization of the τ^- from the distribution of its most prominent subsequent decay modes.

All the polarization components are sensitive to the scalar coupling S_L and the tensor coupling T_L. Besides, the transverse polarization $P_T^{D^*}$ is also sensitive to the vector coupling V_R. The longitudinal and transverse polarizations are more sensitive to T_L in the case of $\overline{B}^0 \to D^*\tau^-\overline{\nu}_\tau$, but more to S_L in the case of $\overline{B}^0 \to D\tau^-\overline{\nu}_\tau$. $P_N^{D^*}$ is equally sensitive to T_L and S_L, while P_N^D is much more sensitive to S_L than to T_L. The normal polarization can reach about ± 0.8 in $\overline{B}^0 \to D\tau^-\overline{\nu}_\tau$ if S_L is present, and about ± 0.2 in other cases. These observations may provide some insights to look for NP in the decays $\overline{B}^0 \to D^{(*)}\tau^-\overline{\nu}_\tau$.

ACKNOWLEDGMENTS

The authors thank the Heisenberg-Landau Grant for providing support for their collaboration. M. A. I. acknowledges the financial support of the PRISMA Cluster of Excellence at the University of Mainz. M. A. I. and C. T. T. greatly appreciate the warm hospitality of the Mainz Institute for Theoretical Physics (MITP) at the University of Mainz.

APPENDIX: HELICITY AMPLITUDES

In this appendix, we express the helicity amplitudes used in the main text in terms of the invariant form factors defined in Eq. (33). A detailed derivation of these relations can be found in our recent paper [5].

For the $\overline{B}^0 \to D$ transition:

$$H_t = \frac{1}{\sqrt{q^2}}(PqF_+ + q^2F_-), \qquad H_0 = \frac{2m_1|\mathbf{p_2}|}{\sqrt{q^2}}F_+, \qquad H_P^S = (m_1+m_2)F^S, \qquad H_T = \frac{2m_1|\mathbf{p_2}|}{m_1+m_2}F^T, \tag{A1}$$

where $|\mathbf{p_2}| = \lambda^{1/2}(m_1^2, m_2^2, q^2)/2m_1$ is the momentum of the daughter meson.

For the $\overline{B}^0 \to D^*$ transition:

$$\begin{aligned}
H_0 &= \frac{-Pq(m_1^2-m_2^2-q^2)A_0 + 4m_1^2|\mathbf{p_2}|^2A_+}{2m_2\sqrt{q^2}(m_1+m_2)},\\
H_t &= \frac{m_1|\mathbf{p_2}|(Pq(-A_0+A_+)+q^2A_-)}{m_2\sqrt{q^2}(m_1+m_2)},\\
H_\pm &= \frac{-PqA_0 \pm 2m_1|\mathbf{p_2}|V}{m_1+m_2},\\
H_V^S &= \frac{m_1}{m_2}|\mathbf{p_2}|G^S,\\
H_T^\pm &= -\frac{1}{\sqrt{q^2}}[(m_1^2-m_2^2 \pm 2m_1|\mathbf{p_2}|)G_1^T + q^2G_2^T],\\
H_T^0 &= -\frac{1}{2m_2}\left[(m_1^2+3m_2^2-q^2)G_1^T + (m_1^2-m_2^2-q^2)G_2^T - \frac{4m_1^2|\mathbf{p_2}|^2}{(m_1+m_2)^2}G_0^T\right].
\end{aligned} \tag{A2}$$

The dependence of the helicity amplitudes and the invariant form factors on q^2 have been omitted for simplicity.

[1] J. Lees *et al.* (*BABAR* Collaboration), Phys. Rev. Lett. **109**, 101802 (2012).
[2] M. Huschle *et al.* (Belle Collaboration), Phys. Rev. D **92**, 072014 (2015).
[3] Y. Sato *et al.* (Belle Collaboration), Phys. Rev. D **94**, 072007 (2016).
[4] R. Aaij *et al.* (LHCb Collaboration), Phys. Rev. Lett. **115**, 111803 (2015); **115**, 159901(E) (2015).
[5] M. A. Ivanov, J. G. Körner, and C. T. Tran, Phys. Rev. D **94**, 094028 (2016).
[6] A. Crivellin, C. Greub, and A. Kokulu, Phys. Rev. D **86**, 054014 (2012).
[7] D. Becirevic, N. Kosnik, and A. Tayduganov, Phys. Lett. B **716**, 208 (2012).
[8] M. De Vito and P. Santorelli, Eur. Phys. J. C **40**, 193 (2005).
[9] U. Nierste, S. Trine, and S. Westhoff, Phys. Rev. D **78**, 015006 (2008).
[10] R. N. Faustov and V. O. Galkin, Mod. Phys. Lett. A **27**, 1250183 (2012).
[11] A. Celis, M. Jung, X. Q. Li, and A. Pich, J. High Energy Phys. 01 (2013) 054.
[12] P. Biancofiore, P. Colangelo, and F. De Fazio, Phys. Rev. D **87**, 074010 (2013).
[13] M. Duraisamy and A. Datta, J. High Energy Phys. 09 (2013) 059.
[14] Y. Sakaki, M. Tanaka, A. Tayduganov, and R. Watanabe, Phys. Rev. D **88**, 094012 (2013).
[15] M. Duraisamy, P. Sharma, and A. Datta, Phys. Rev. D **90**, 074013 (2014).
[16] L. Calibbi, A. Crivellin, and T. Ota, Phys. Rev. Lett. **115**, 181801 (2015).
[17] A. Greljo, G. Isidori, and D. Marzocca, J. High Energy Phys. 07, (2015) 142.
[18] M. Bauer and M. Neubert, Phys. Rev. Lett. **116**, 141802 (2016).
[19] S. Fajfer and N. Kosnik, Phys. Lett. B **755**, 270 (2016).
[20] R. Barbieri, G. Isidori, A. Pattori, and F. Senia, Eur. Phys. J. C **76**, 67 (2016).
[21] R. Barbieri, C. W. Murphy, and F. Senia, Eur. Phys. J. C **77**, 8 (2017).
[22] S. M. Boucenna, A. Celis, J. Fuentes-Martin, A. Vicente, and J. Virto, Phys. Lett. B **760**, 214 (2016).
[23] X. Q. Li, Y. D. Yang, and X. Zhang, J. High Energy Phys. 08, (2016) 054.
[24] S. Nandi, S. K. Patra, and A. Soni, arXiv:1605.07191.

[25] A. K. Alok, D. Kumar, S. Kumbhakar, and S. U. Sankar, arXiv:1606.03164.
[26] N. Deshpand and X. G. He, arXiv:1608.04817.
[27] C. S. Kim, G. Lopez-Castro, S. L. Tostado, and A. Vicente, Phys. Rev. D **95**, 013003 (2017).
[28] D. Bardhan, P. Byakti, and D. Ghosh, J. High Energy Phys. 01 (2017) 125.
[29] R. Dutta and A. Bhol, arXiv:1611.00231.
[30] L. Wang, J. M. Yang, and Y. Zhang, arXiv:1610.05681.
[31] A. Celis, M. Jung, X. Q. Li, and A. Pich, arXiv:1612.07757.
[32] S. Bhattacharya, S. Nandi, and S. K. Patra, arXiv:1611.04605.
[33] D. Becirevic, S. Fajfer, N. Kosnik, and O. Sumensari, Phys. Rev. D **94**, 115021 (2016).
[34] D. Becirevic, N. Kosnik, O. Sumensari, and R. Zukanovich Funchal, J. High Energy Phys. 11, (2016) 035.
[35] S. Hirose *et al.* (Belle Collaboration), arXiv:1612.00529.
[36] H. Na, C. M. Bouchard, G. P. Lepage, C. Monahan, and J. Shigemitsu (HPQCD Collaboration), Phys. Rev. D **92**, 054510 (2015); **93**, 119906(E) (2016).
[37] J. A. Bailey *et al.* (MILC Collaboration), Phys. Rev. D **92**, 034506 (2015).
[38] S. Aoki *et al.*, arXiv:1607.00299.
[39] S. Fajfer, J. F. Kamenik, and I. Nisandzic, Phys. Rev. D **85**, 094025 (2012).
[40] R. Garisto, Phys. Rev. D **51**, 1107 (1995).
[41] Y. S. Tsai, Nucl. Phys. B, Proc. Suppl. **55**, 293 (1997).
[42] G. H. Wu, K. Kiers, and J. N. Ng, Phys. Rev. D **56**, 5413 (1997).
[43] J. P. Lee, Phys. Lett. B **526**, 61 (2002).
[44] M. Tanaka and R. Watanabe, Phys. Rev. D **82**, 034027 (2010).
[45] A. Datta, M. Duraisamy, and D. Ghosh, Phys. Rev. D **86**, 034027 (2012).
[46] M. Tanaka and R. Watanabe, Phys. Rev. D **87**, 034028 (2013).
[47] S. Bhattacharya, S. Nandi, and S. K. Patra, Phys. Rev. D **93**, 034011 (2016).
[48] D. Becirevic, S. Fajfer, I. Nisandzic, and A. Tayduganov, arXiv:1602.03030.
[49] M. A. Ivanov, J. G. Körner, and C. T. Tran, Phys. Rev. D **92**, 114022 (2015).
[50] One of the authors of the present paper (J.G.K.) records his contentment that the values $\langle P_L^\tau \rangle = 0.33$ $(B \to D)$ and $\langle P_L^\tau \rangle = -0.53$ $(B \to D^*)$ calculated in the early paper [63] are quite close to those calculated in [49].
[51] J. G. Körner and D. Pirjol, Phys. Rev. D **60**, 014021 (1999).
[52] S. Groote, W. S. Huo, A. Kadeer, and J. G. Körner, Phys. Rev. D **76**, 014012 (2007).
[53] M. Fischer, S. Groote, J. G. Körner, and M. C. Mauser, Phys. Rev. D **67**, 113008 (2003).
[54] B. K. Bullock, K. Hagiwara, and A. D. Martin, Nucl. Phys. **B395**, 499 (1993).
[55] R. Alonso, A. Kobach, and J. M. Camalich, Phys. Rev. D **94**, 094021 (2016).
[56] G. Mahlon and S. J. Parke, Phys. Rev. D **53**, 4886 (1996).
[57] S. J. Parke and Y. Shadmi, Phys. Lett. B **387**, 199 (1996).
[58] G. Mahlon and S. J. Parke, Phys. Lett. B **411**, 173 (1997).
[59] S. Groote, J. G. Körner, B. Melic, and S. Prelovsek, Phys. Rev. D **83**, 054018 (2011).
[60] L. Kaldamäe, S. Groote, and J. G. Körner, Phys. Rev. D **94**, 114003 (2016).
[61] J. G. Körner and G. A. Schuler, Z. Phys. C **38**, 511 (1988); **41**, 690(E) (1989).
[62] J. G. Körner and G. A. Schuler, Phys. Lett. B **231**, 306 (1989).
[63] J. G. Körner and G. A. Schuler, Z. Phys. C **46**, 93 (1990).
[64] A. Faessler, T. Gutsche, M. A. Ivanov, J. G. Körner, and V. E. Lyubovitskij, Eur. Phys. J. direct C **4**, 18 (2002).
[65] T. Gutsche, M. A. Ivanov, J. G. Körner, V. E. Lyubovitskij, and P. Santorelli, Phys. Rev. D **88**, 114018 (2013).
[66] T. Gutsche, M. A. Ivanov, J. G. Körner, V. E. Lyubovitskij, P. Santorelli, and N. Habyl, Phys. Rev. D **91**, 074001 (2015); **91**, 119907(E) (2015).
[67] T. Branz, A. Faessler, T. Gutsche, M. A. Ivanov, J. G. Körner, and V. E. Lyubovitskij, Phys. Rev. D **81**, 034010 (2010).
[68] M. A. Ivanov, J. G. Körner, S. G. Kovalenko, P. Santorelli, and G. G. Saidullaeva, Phys. Rev. D **85**, 034004 (2012).
[69] M. A. Ivanov and C. T. Tran, Phys. Rev. D **92**, 074030 (2015).
[70] I. Caprini, L. Lellouch, and M. Neubert, Nucl. Phys. **B530**, 153 (1998).
[71] C. Bourrely, L. Lellouch, and I. Caprini, Phys. Rev. D **79**, 013008 (2009); **82**, 099902(E) (2010).